ISSN-2230-9659

# Local Symmetry and Unstability in Single-Molecule Rhodamine 6G Raman Scattering on Silver Nanocrystal Aggregates


**Sarita Rani**

Research Scholar, Singhania University

Rajasthan, India



## Abstract

Surface enhanced Raman scattering (SERS) from Rhodamine 6G adsorbed on small, optically resolvable aggregates of silver nanoparticles is detectable at the single-molecule level. The signal fluctuates on a second time scale, presumably due to movement of the molecule in to and out of the SERS active "hot spots". The depolarization of the signal is found to be independent of the unstabilitys, to vary from one spot to the next, and to be highly dependent on the direction of the incident electric field. The "SERS continuum" dominates the signal and is assumed to arise from electronic Raman processes in the metal that are triggered by chemisorption of the molecule in the hot spot. The source of the Raman signal is therefore highly localized around the hot spot. The local structure determines the depolarization properties and is often extremely anisotropic. Conversely, the Rayleigh scattering does not depend on the molecule or the hot spot and is delocalized over the whole

ISSN-2230-9659

aggregate, which is always found to be highly isotropic. The Rayleigh scattering therefore does not fluctuate and is always highly polarized.

## Introduction:

From the early work on surface enhanced Raman scattering (SERS), it is known that nanometer scale roughness is necessary for a surface to exhibit SERS.1 Until recently, all studies involved large (micrometer scale) surface areas, with many adsorbed molecules in differing environments contributing to the signal. These experiments only probe a surface-averaged enhancement, which in the best situations reaches as high as 106 for the first monolayer, corresponding roughly to a cross section *ó* of 10-23 cm2 per mode for a molecule without a molecular electronic resonance effect. Within the past few years, however, experiments have been undertaken to probe the microscopic nature of enhancement for individual molecules. These include NSOM experiments on extended fractal aggregates of silver particles2 and far-field microscope experiments on optically resolvable, supported stationary aggregates3-8 and dilute aqueous colloids.9 In some cases, individual molecules are observed with apparent *ó* far larger than 10-23 cm2.

To date the largest reported *ó* occurs for Rhodamine 6G (R6G) molecules adsorbed from aqueous solution onto small aggregates of _50 nm silver nanocrystals. This reflects a SERS effect combined with a R6G molecular resonance Raman enhancement. At 514.5 nm, *ó* ) 2 _ 10-14 cm2,7 and at 532.0 nm (near the peak of the molecular absorption), *ó* ) 10-13 cm2.6 Here, the quoted *ó* is a net cross section for all Raman peaks and underlying continuum in the SERS spectrum. Rayleigh (plasmon) scattering spectra and direct AFM examination show that these huge cross sections ("hot spots") occur *not* in single nanocrystals, but in compact (nonfractal) aggregates of several individual _50 nm silver nanocrystals.7 For some time, it has been understood that especially large enhancements occur in junctions and internal cavities of aggregated silver particles.1,10,11

ISSN-2230-9659

The evidence for single-molecule detection rests on two observations: (1) the low adsorbate-to-particle ratios used in the experiments make it unlikely that there could be more than one adsorbate per aggregate, and (2) an on-off blinking behavior indicative of single-molecule dynamics is found. Periods of several seconds can occur when there is no Raman intensity, followed by long periods when the Raman intensity returns. This on-off cycling can continue for several minutes, until the signal finally bleaches out permanently from the intense fields present. During the "on" periods, the SERS intensity fluctuates on a second time scale, with some unstability in the spectral profile. The unstability rate increases linearly with laser power.6 Thus, the unstabilitys are not thermal, but driven by photophysical dynamics.

The observed unstabilitys form the basis of our experiments in which the intensities of the two orthogonal polarizations of the Raman scattering are followed simultaneously. This represents the first such measurement in the single-molecule Raman field. The depolarization is found to be independent of the unstabilitys, to vary from one hot spot to the next, and to depend strongly on the direction of the laser field with respect to the aggregate axes. The results are interpreted in terms of the motion of the adsorbate and the optical anisotropy of the local site.

## Experiment:

Our procedures, sample preparation, and inverted microscope (Nikon TE300) based apparatus have been described previously.7 Briefly, S-polarized laser light at grazing incidence (514.5 nm, ~100 W $cm^{-2}$, NA 0.004) illuminates the sample on a stage that is capable of being rotated about the vertical *z* laboratory axis. The silver nanocrystal aggregates are stationary on the coverslip under ambient conditions. The scattered light is collected through the coverslip along the vertical optical axis (~90° scattering geometry, air objective, NA 0.60) and focused onto a beam displacing prism

ISSN-2230-9659

(Melles Griot 03PPD312) at the side port of the microscope. The prism displaces the S-polarized light relative to the P-polarized light, producing separate images

of the scattering center for each polarization.

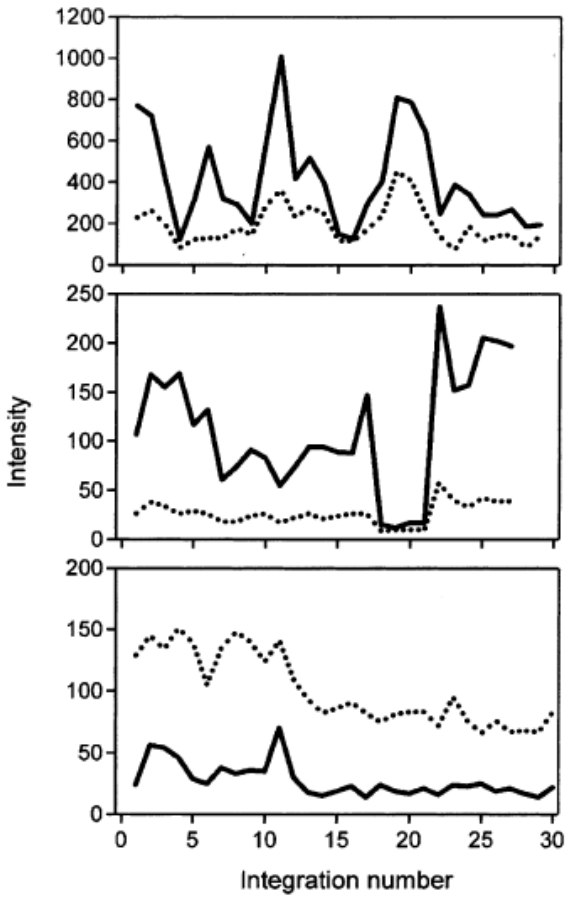


**Figure 1.** Time dependence of the intensities of the S- (solid) and P- (dotted) polarized Raman scattering from three different SERSactive aggregates. The scattering is excited by 514.5 nm, S-polarized light; all the Stokes (and anti-Stokes) shifted light contributes to the signal. The integrations are 1 s long and taken continuously at 2s intervals.

ISSN-2230-9659

The intermediate images are relayed through a notch filter (to reject the Rayleigh scatter) and focused onto a liquid nitrogen cooled CCD detector, allowing the two polarizations to be monitored simultaneously. The microscope is also equipped with a dark-field condenser for imaging. Typically, the intensity of the Raman scattered light from a single "hot spot" is followed through 1 s integrations taken at 2 s intervals.

## Results and Discussion:

In all we studied a dozen or so intense R6G SERS signals. Figure 1 shows the intensity of the S- and P-polarized Raman scatter for a sequence of about thirty integrations from three separate, representative particles. The incident field is arbitrarily oriented with respect to the aggregate axes in the plane of the coverslip. Intensity unstabilitys on the second time scale are clearly seen in all of these plots. Moreover, in the second plot an interval (18-21) with essentially zero intensity is present, corresponding to an "off" period in the above-mentioned onoff blinking behavior. The blinking behavior, and more generally the unstabilitys, indicates that the signal is from a single molecule. It is clearly seen from these plots that the S- and P-polarized scatter fluctuate together; that is, their intensities are strongly correlated. For some particles the S-polarized scatter is stronger than the P-polarized scatter (first and second plots), but for others the P-polarized scatter is stronger (third plot). Finally, for some of the particles, such as that in the third plot, in addition to the random unstabilitys there is also a consistent bleaching with time. The polarization state is parametrized by F ) (*I*SS - *I*SP)/(*I*SS + *I*SP), where *I*SS and *I*SP are the intensities of the S- and P-polarized Raman scatter, given S-polarized incident light.

ISSN-2230-9659

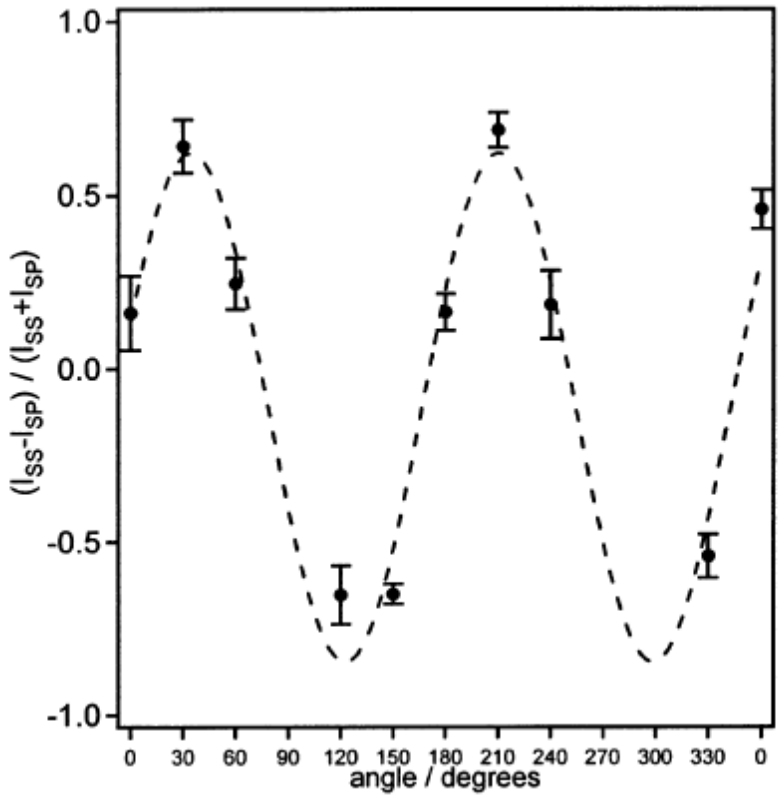


**Figure 2.** Angle dependence of the polarization parameter $\rho$ for a representative SERS-active aggregate. The data are collected under the same conditions described in Figure 1. Ten integrations are taken at each angle, with 30□ increments. A polarization parameter equal to 1 indicates that the scattering is completely polarized and -1 indicates that it is completely depolarized. The error bars represent $\pm 1\sigma_\rho$.

The strong correlations between the S- and P-polarized scattering intensities, as seen in Figure 1, are reflected in small standard deviations *ó*F for F, which are found to be between about 0.05 and 0.15. Rayleigh scattering at 514.5 nm is similarly investigated by removing the notch filter and lowering the integration time. As previously reported, the Rayleigh scattered light does not show any unstabilitys. In contrast to the SERS scattering, we find the Rayleigh scatter is always highly polarization preserving (i.e., S-polarized).

To explore SERS structural symmetry by scattering depolarization, we rotate the aggregate in the *x*,*y* horizontal plane. Following normal theory, we interpret our data using ***p*** ) R***Ae***, where ***p*** is the radiating dipole and ***e*** is the incident laser electric field. If ***p*** has the same direction as

ISSN-2230-9659

***e***, then the scattering is polarized. R***A*** is the polarizability tensor (not rotationally averaged), where R is a scalar and ***A*** is a second-rank tensor. (The polarizability tensor has been split up this way to conform with the experimental results.) There are different polarizability tensors R***A*** for SERS and Rayleigh scattering. Strictly speaking, this model applies to a scattering center that is much smaller than the wavelength of the incident light and that is reradiating at a single frequency, neither of which is the case here.12 The model can, however, be used to qualitatively understand these results. The fluctuating intensity of the Raman scattering is contained within R, whereas the nonfluctuating polarization properties are determined by ***A***. Depolarization, i.e., the presence of P-polarized scatter, indicates that ***A*** has nonzero off-diagonal matrix elements. Specifically, with the incident field polarized in the *x* direction and the scattered light being collected in the *z* direction, *Axx* is responsible for polarized scatter and *Ayx* for depolarized scatter. Rotation of the scattering center about the *z* axis will mix the *Axx*, *Ayy*, *Axy*, and *Ayx* elements.

We rotate the stage about *z* and bring the aggregate back onto the optical axis of the collection lens using the stage *x*,*y* motions while following the aggregate under dark-field illumination. Figure 2 shows the polarization parameter F measured for a sequence of angles of rotation, with ten integrations taken at each angle. We observe that F is independent of the unstabilitys at all angles.

| | $A_{ij}\,(0^\circ)$ | $\rho(\theta)$ |
|---|---|---|
| isotropic | $A_{xx} = A_{yy} \neq 0$<br>$A_{xy} = A_{yx} = 0$ | 1 |
| anisotropic (extreme) | $A_{xx} \neq 0$<br>$A_{yy} = A_{xy} = A_{yx} = 0$ | $\cos 2\theta$ |
| off-diagonal symmetric | $A_{xy} = A_{yx} \neq 0$<br>$A_{xx} = A_{yy} = 0$ | $-\cos 4\theta$ |
| asymmetric (extreme) | $A_{xy} \neq 0$<br>$A_{xx} = A_{yy} = A_{yx} = 0$ | $\cos 2\theta$ |

ISSN-2230-9659

TABLE 1: Representative Forms of the Scattering Tensor and Corresponding Angle Dependent Polarization Parameters.

The data clearly shows that strongly depolarized Raman scattering $(\rho \approx -1)$ can be made highly polarized $(\rho \approx 1)$ by rotating the aggregate. Note that the high NA of the objective used to collect scattered light affects the maximum value of $\rho$. In the small aperture limit, on which the above analysis was based, only the projection of the radiating dipole onto the plane of the coverslip is important. However, with a large aperture one can also "see" the out-of-plane component of the radiating dipole. For a stationary scattering center the out-of-plane component would have to be about 1.4 times the in-plane component to account for the observed extrema of $\rho \sim \pm 0.7$, as calculated following Axelrod's analysis13 with an NA of 0.6. Although this is possible, there could be other causes of the observed extrema as well. One possibility is that there are higher moments contributing to the signal (e.g. quadrupolar Raman), which would be described by different tensors. The wavelength dependence of the polarizability tensor may also contribute and will be discussed more below when we consider the dominant contributions to the signal. Finally, it is also possible that there are dynamics happening on a shorter time scale, leading to a diminished F. For example, the molecule may be rapidly rotating about some axis. It is found that the scattering from any particle that shows depolarization can be made polarized by suitable rotations; however, some particles do not show any significant depolarization regardless of the angle. Although intermediate cases were not found, the difficulty in collecting complete data sets (due to irreversible bleaching of the signal) limits the size of the sample that can be used to characterize all possible behaviors. The polarization of the Rayleigh scattering is similarly investigated. It is found that the Rayleigh scattering is always highly polarized, regardless of the angle. This is true even for particles that show strongly depolarized Raman scattering.

We compare these results for $\rho(\theta)$ with those calculated for representative forms of $\boldsymbol{A}$ (see Table 1). For the isotropic case, $\rho$ is independent of the angle of rotation, implying that the scattering is always polarization preserving regardless of the angle. This is experimentally

ISSN-2230-9659

observed for all of the Rayleigh scattering and for some of the Raman. For the extreme anisotropic case, $\rho$ cycles in a sinusoidal fashion from 1 to -1 and back to 1 with each 180° rotation. A milder anisotropy $(A_{xx} \neq A_{yy} \neq 0)$ leads to $\rho(\theta)$ not going all the way to -1 and not varying as a simple sinusoid. The symmetric off-diagonal case leads to similar results as the extreme anisotropic one except with a 90° period. The experimental SERS polarization for most spots investigated, including the one shown in Figure 2, is consistent with the extreme anisotropic form of ***A***; that is, $\rho$ varies such as $\cos(2\theta)$. Other forms of ***A*** are investigated numerically. No other symmetric form is found that fits the observed data. Asymmetric forms should not be ruled out a priori (they are found for example in normal resonant Raman processes), and indeed asymmetric forms are found that produce the observed angular dependence of $\rho$ (see Table 1).

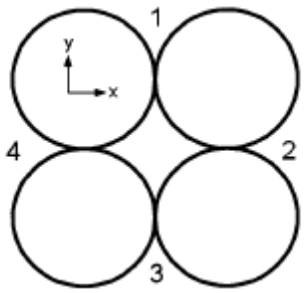


**Figure 3.** Schematic representation of the difference between Rayleigh and Raman scattering from SERS-active aggregates. The Rayleigh

scattering is delocalized over the whole aggregate, which, in this example, is isotropic due to the 4-fold axis of symmetry. (Formally, an axis of symmetry of order three or higher ensures that the tensor is isotropic in the plane perpendicular to that axis.) Conversely, the Raman scattering is highly localized at one of the junctions, which is highly anisotropic.

ISSN-2230-9659

This however requires extreme asymmetry, which cannot easily be justified on physical grounds. It is more likely that the observed behavior is due to an extreme anisotropy. In summary, some of the particles show highly depolarized Raman scattering that is consistent with an anisotropic scattering center; others show more isotropic, polarized scatter. The Rayleigh scattering is always highly polarized, indicating that it is from an isotropic scattering center.

## Junction and Cavity Sites for Raman Depolarization:

Consider the heuristic tutorial model in Figure 3. Four silver nanocrystals form a symmetric square (*D*4*h* symmetry) with four junctions. Only one junction has an R6G molecule. We plausibly assume that the induced SERS radiating dipole ***p*** (representing both continuum and totally symmetric R6G vibrational modes) is parallel to and scales with the local enhanced field ***e*loc** in his one junction. In this model the ***A*** part of the SERS polarizability $\alpha_A$ relates the magnitude and direction of ***e*loc** in just one junction to the direction of the incident S-polarized laser field ***e***. Calculation of $\alpha_A$, based on the true structure of an aggregate, could be done using numerical methods within Mie theory14 or via the discrete dipole approximation.15 For the simplest case of two spherical nanocrystals forming a dimer, $\alpha_A$ is known from analytical solutions including retardation. The dimer has a very strong transition dipole along the internuclear axis and a weak perpendicular dipole. The axial transition dipole creates a huge axial ***e*loc** for ***e*** polarized only along this axis.10 Using this result, we anticipate that if ***e*** is polarized along *x* in the aggregate, there will be intense ***e*loc** in junctions 1 and 3, and if polarized along *y*, intense ***e*loc** in junctions 2 and 4. If the molecule is in junction 1, the resulting SERS tensor ***A*** will be strongly anisotropic with only *Axx* large.

Rayleigh scattering represents the coherent optical polarization of the metallic electrons in the aggregate. In general, the observed isotropic Rayleigh scattering is consistent with the previous observation that the aggregates are compact, threedimensional structures. In

ISSN-2230-9659

our *D*4*h* model, the Rayleigh tensor will be isotropic because of the 4-fold symmetry axis of the aggregate. Note that although we have not measured the rotational variation of Rayleigh and SERS intensity, this model predicts that the Rayleigh intensity is independent of $\theta$, whereas the SERS intensity varies strongly with $\theta$. This is consistent with the previously measured absence-of-correlation between Rayleigh and Raman intensities for arbitrary directions.7 We found a few SERS signals to be strongly polarized for all angles, as might be the case for a molecule in the symmetrical center cavity of Figure 3. Note that a tetrahedral aggregate such as considered by Liver et al also has a symmetrical central cavity as well as junction sites.11 The possible existence of single molecule SERS from these sites needs to be more carefully investigated.

This single molecule SERS signal is dominated by the continuum underlying the sharp Raman lines.7 Our depolarization results show that this continuum is generated by a local process not having the full symmetry of the aggregate. This was also concluded earlier from the fact that the continuum and Raman lines blink on and off together. We suggest that this continuum is electronic Raman scattering of the local, coherently driven metallic electrons at the junction, whose polarization direction is the same as ***e*loc**. Electronic Raman scattering, creating excited electrons above the Fermi surface, is not a general property of silver crystals. In our experiment, only those aggregates that show R6G Raman also show continuum scattering. In a simple Fermi gas with well-defined electronic momenta, electronic Raman scattering is forbidden by momentum conservation except very close to the laser line. The momentum transferred to the electron-hole pair in optical scattering is only large enough to create an electron-hole pair of a few cm-1 energy above the Fermi surface. However, in "dirty metals" the momentum selection rules are relaxed by scattering off defects, and electronic Raman scattering over a wide energy range becomes possible.16,17 Thus strong electronic Raman scattering in silver is associated with defects, on rough, cold deposited silver films and on the surfaces of silver nanocrystals formed by ion implantation into silica.18 We suggest that the adsorbed R6G molecule acts as a defect. Exchange coupling

ISSN-2230-9659

between the excited metallic electrons and the R6G molecule causes both the continuous electronic Raman and the discrete molecular Raman. We quantitatively explore this idea in a following publication.

## Conclusion:

The SERS scattering intensity fluctuates due to motions of the molecule in and out of the hot spot and is highly localized around it. The hot spot can be highly anisotropic leading to depolarization of the scattering for some of the SERS active aggregates. The anisotropy of the hot spot is a property of the aggregate and does not depend on motion of the molecule. Therefore, the polarization of the Raman scattering does not fluctuate like the intensity does. The Rayleigh scattering, on the other hand, does not depend on the hot spot or the chemisorbed molecule. It is delocalized over the entire aggregate, which is always found to be isotropic. Hence, the Rayleigh scattering is always polarization preserving and does not fluctuate.



## References and Notes:

(1) For reviews see Moskovits, M. *Re*V. *Mod. Phys.* **1985**, *57*, 783; Otto, A.; Mrozek, I.; Grabhorn, H.; Akemann, W. *J. Phys.: Condens. Mater.* **1992**, *4*, 1143.

(2) Markel, V. A.; Shalaev, V. M.; Zhang, P.; Huynh, W.; Tay, L.; Haslett, T. L.; Moskovits, M. *Phys. Re*V. *B* **1999**, *59*, 10 903.

(3) Nie, S.; Emory, S. R. *Science* **1997**, *275*, 1102.

(4) Doering, W.; Nie, S. *J. Phys. Chem. B* **2002**, *106*, 311.

ISSN-2230-9659

(5) Xu, H.; Bjerneld, E. J.; Ka¨ll, M.; Bo¨rjesson, L. *Phys. Re*V. *Lett.* **1999**, *83*, 4357.

(6) Weiss, A.; Haran, G. *J. Phys. Chem. B* **2001**, *105*, 12 348.

(7) (a) Michaels, A. M.; Nirmal, M.; Brus, L. E. *J. Am. Chem. Soc.* **1999**, *121*, 9932. (b) Michaels, A. M.; Jiang, J.; Brus L. *J. Phys. Chem. B* **2000**, *104*, 11 965.

(8) Meixner, A.; Vosgrone, T.; Sackrow, M. *J. Lumin.* **2001**, *94-95*, 147.

(9) Kneipp, K.; Wang, Y.; Kneipp, H.; Perelman, L. T.; Itzkan, I.; Dasari, R.; Feld, M. S. *Phys. Re*V. *Lett.* **1997**, *78*, 1667.

(10) Inoue, M.; Ohtaka, K. *J. Phys. Soc. Jpn.* **1983**, *52*, 3853.

(11) Liver, N.; Nitzan, A.; Gersten, J. *Chem. Phys. Lett.* **1984**, *111*, 449.

(12) Long, D. A. *Raman Spectroscopy*; McGraw-Hill: New York, 1977.

(13) Axelrod, D. *Method Cell Biol.* **1989**, *30*, 333.

(14) Quinten, M. *Appl. Phys. B* **2001**, *73*, 245.

(15) Schatz, G. *Theochem* **2001**, *573*, 73.

(16) Zawadowski, A.; Cardona, M. *Phys. Re*V. *B* **1990**, *42*, 10732.

ISSN-2230-9659

(17) Itai, K. *Phys. Re*V. *B* **1992**, *45*, 707.

(18) Portales, H.; Duval, E.; Saviot, L.; Fujii, M.; Sumitomo, M.; Hayashi, S. *Phys. Re*V. *B* **2001**, *63*, 233 402.